Low Temperature STM/STS, Standard AFM and XPS of Local MgB$_x$ Phases

B. Strzelczyk[a,*], W. Kempiński[a,†], M. Wróblewski[b], B. Susła[b], J. Piekoszewski[c], Z. Werner[c], M. Barlak[c], J. Martinek[a], M. Błaszyk[a], Sz. Maćkowiak[a,b], Z. Trybuła[a], Sz. Łoś[a] and M. Kempiński[d]

[a]Institute of Molecular Physics, Polish Academy of Sciences, M. Smoluchowskiego 17, 60-179 Poznań, Poland

[b]Institute of Physics, Poznań University of Technology, Nieszawska 13A, 60-965 Poznań, Poland

[c]The Andrzej Sołtan Institute for Nuclear Studies, 05-400 Otwock/Świerk, Poland

[d]Faculty of Physics, Adam Mickiewicz University, Umultowska 85, 61-614 Poznań, Poland

Low temperature scanning tunneling microscopy/ scanning tunneling spectroscopy, room temperature atomic force microscopy and X-ray photoelectron spectroscopy of the boron ions implanted into the magnesium substrate were performed in order to get information about the local superconducting behavior of thin MgB$_x$ film. Results confirm the island superconductivity far from the percolation threshold of the bulk superconducting MgB$_2$ sample.

PACS numbers: 74.70.Ad, 74.78.−w, 68.37.Ef, 74.55.+v

1. Introduction

For many years the superconducting properties of the magnesium diborate have been the subject of the intensive studies of different kind of samples: bulk material [1], monocrystalline MgB$_2$ [2, 3], polycrystalline (wire, tape) [4] or thin films [5]. Obtaining the good quality thin film of MgB$_2$ is a great challenge from the application point of view for this superconducting material [6–8]. One of the most intriguing problems for this material is its energy gap. Based on the scanning tunneling spectroscopy (STS) method this problem is discussed [9–13] also with the two different energy gaps observed with directional STS [14].

In our earlier experiments thin layers of MgB$_x$ were obtained with the use of ion implantation and plasma pulse treatment method [15–20]. Samples were prepared in order to define evolution of the superconducting phases after B ions implantation into the Mg substrate or vice versa [15, 16]. Much effort has been put into collecting information about the local composition of the superconducting islands [15–17]. To get more information on the electronic properties of the surface and the layers right below, the low temperature scanning tunneling microscopy and spectroscopy (LT STM/STS) methods were used as well as the *ex situ* room temperature atomic force microscopy (AFM) and the X-ray photoelectron spectroscopy (XPS) investigations over the MgB$_x$ obtained by the B$^+$ implantation into the Mg substrate.

2. Experimental

LT STM/STS were performed using a commercial scanning tunneling microscope — CryoSXM, Omicron. The Pt–Ir STM tips were used, so the tunneling junction between the tip and the sample in the superconducting state was of the SIN type (superconductor/insulator/normal metal). The microscope was placed inside the home made cryostat, filled with the liquid helium. Microscope workspace was filled with the helium gas under the atmospheric pressure to ensure the heat transfer between the sample and the cooling medium. It allows to cool down the microscope workplace down to ≈ 5 K without lowering the pressure below the atmospheric value — the so-called pumping procedure. After the helium pumping procedure the temperature close to 2 K can be reached. Temperature was measured using a semiconductor-based Cernox thermometer. To get the information about the energy gap for MgB$_x$, STS mode was used. STS measurements of the MgB$_x$ were taken within the temperature range of 9–13 K during the slow self heating of the system. The measurements were performed in the temperature far below the critical point ($T_c = 31$ K) where the studied material is well defined as a superconducting one [15].

Analysis of the chemical composition of the MgB$_x$ was preceded by the XPS measurements. Chemical composition test was performed at a room temperature inside the multipurpose ultrahigh vacuum (UHV) surface analysis system (Prevac) with the base pressure $\approx 5 \times 10^{-10}$ mbar. XPS spectrometer with a X-ray gun (Prevac) — Mg K_α line at 1253 eV, together with the hemispherical photo-

---

* Actual address: Faculty of Physics and Applied Computer Science, AGH University of Science and Technology, Kraków, Poland

† corresponding author; e-mail: `wojkem@ifmpan.poznan.pl`

electron energy analyzer (Scienta) was used to determine the photoemission spectra of the tested sample.

3. Chemical composition

The XPS spectrum measured for the MgB_x sample is shown in Fig. 1. The rich spectrum shows a few peaks related to the elements present on the sample surface and some artifacts related to the sample surroundings (e.g. the sample holder). These artifacts such as Mo, Ta or W peaks can appear due to the very small sample diameter and the relatively large area of the data collection.
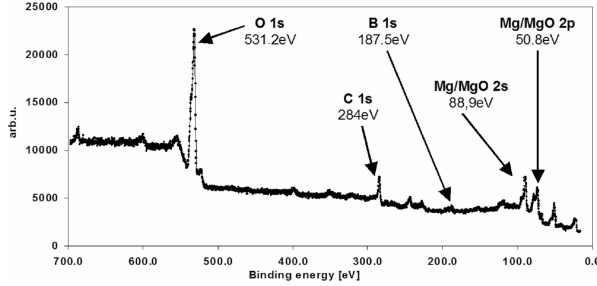

Fig. 1. XPS spectrum of MgB_x sample; arrows indicate peaks connected to the elements and compounds present on the sample surface. Other visible peaks are the artifacts coming from the sample surroundings.

Peaks related to the composition of the MgB_x sample surface are indicated with arrows in Fig. 1. The XPS spectrum reveals large peaks of Mg $2s$ at 88.9 eV and Mg $2p$ at 50.8 eV peaks together with a tiny boron $1s$ peak at 187.5 eV. Energies of the Mg peaks are related to the magnesium oxide rather than the metallic Mg. Such small B $1s$ peak indicates that magnesium boride compound is surely not a stoichiometric MgB_2. Metallic magnesium not bounded into MgB_x compound is strongly oxidized, which is revealed by the presence of a very large O $1s$ at 529.8 eV peak, shifted from the atomic oxygen energy of 531.8 eV, which is characteristic of oxygen in MgO. Moreover, the sample surface is strongly contaminated by carbon (C $1s$ at 284 eV).

4. STM/STS of MgB_x

Most STS experiments use the "current-imaging tunneling spectroscopy" (CITS), introduced by Hamers et al. [21]. CITS images are based on a regular matrix of points distributed over the surface. The tip is scanned over the sample surface with a fixed tunneling resistance, recording the topographic information. At each point of the CITS array, the scan and feedback are interrupted to freeze the tip position. It allows the voltage to be swept to measure $I(V)$ and/or dI/dV, either at a single bias value or over an extended voltage range. The bias voltage is then set back to V_t, the feedback is turned on, and the scanning resumed. The result is a topographic image measured at V_t with simultaneous spectroscopic images

reconstructed from the $I(V)$ and/or dI/dV data. Because the feedback loop is interrupted, V can take any value, even those where $I(V) = 0$. The differential tunneling conductance (dI/dV) spectra provide direct information about local density of states (LDOS) on the sample surface related to their superconducting properties [22].
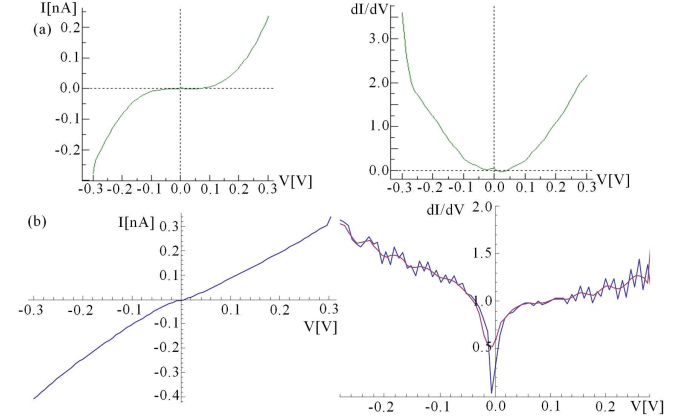

Fig. 2. STS spectra of the MgB_x surface sample: (a) sample in the normal state (room temperature); (b) sample in the superconducting state (9–13 K).

Measurements were performed in CITS mode to collect data from the relatively large area of the sample and the presented spectra are averaged over hundreds of individual curves taken from a few nanometers area. According to the sample preparation method most of the arising superconducting islands are located under the surface and only some of them have a chance to be seen at the surface. Due to this fact obtaining the CITS map of superconducting islands was not possible. STS spectra were obtained in the different places of the MgB_x sample in order to find its superconducting behavior. Characteristic behavior is shown in Fig. 2: $I(V)$ on the left side and dI/dV on the right side of the figure. Figure 2a shows the measurements performed in room temperature and reveals a semiconductor-like shape of the energy gap in the LDOS picture (Fig. 2a, spectrum on the right). Figure 2b represents results obtained in low (9–13 K) temperature (far below T_c of this material [15]). dI/dV curve (Fig. 2b, spectrum on the right) shows the superconducting energy gap with $\Delta \approx 5$ meV measured in FWHM, which indicates a superconducting state of the tested material. The observed spectra do not reveal the presence of the double energy gap which indicates a large disorder on the MgB_x phase [14]. The value of the measured energy gap is larger than the one obtained by Heitmann et al. [23] for epitaxial thin films of the stoichiometric MgB_2 compound. This group reported values within 2.2–2.8 meV range, depending on the temperature.

Difference between the measured value and that reported in the literature may come from several reasons. From the XPS result we know that the sample surface is
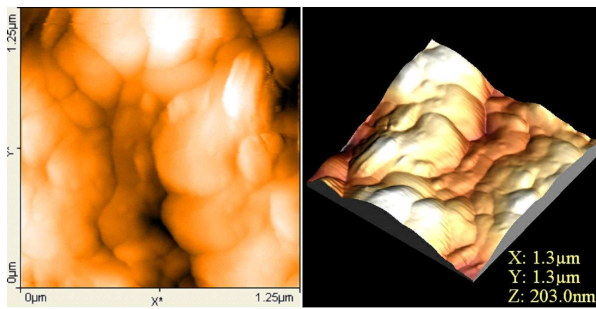
Fig. 3. MgB$_x$ sample surface topography taken with AFM.

strongly oxidized and has a large amount of impurities. Also the MgB$_x$ compound is far from stoichiometry due to the new sample preparation procedure which also creates a large inhomogeneous surface areas. Topography of the sample is presented in Fig. 3 — it reveals the sample surface to be very rough and inhomogeneous.

5. Conclusions

LT STM/STS measurements confirm the presence of the local islands of superconducting structure obtained by the special method of implantation of the B$^+$ ions into the Mg substrate. Topography of the sample studied by the STM and the AFM together with the XPS analysis have shown that the sample surface is rough and inhomogeneous. The obtained results suggest that the simple implantation method could be useful only in case of creation of the superconducting MgB$_x$ islands rather than the smooth continuous MgB$_2$ thin superconducting films. To get the homogeneous MgB$_2$ thin film, additional steps connected with the appropriate surface thermal treatment are necessary [20]. Experiments which can test the superconductivity of MgB$_2$ thin film under the percolation threshold are in preparation.

Acknowledgment

References

[1] Y. Takano, H. Takeya, H. Fujii, H. Kumakura, T. Hatano, K. Togano, *Appl. Phys. Lett.* **78**, 2914 (2001).

[2] M. Xu, H. Kitazawa, Y. Takano, J. Ye, K. Nishida, H. Abe, A. Matsushita, N. Tsujii, G. Kido, *Appl. Phys. Lett.* **79**, 2779 (2001).

[3] S. Lee, H. Mori, T. Masui, Yu. Eltsev, A. Yamamoto, S. Tajima, *J. Phys. Soc. Jpn.* **70**, 2255 (2001).

[4] S. Jin, H. Mavoori, C. Bower, R.B. van Dover, *Nature* **411**, 563 (2001).

[5] W.N. Kang, H.J. Kim, E.M. Choi, C.U. Jung, S.I. Lee, *Science* **292**, 1521 (2001).

[6] N. Peng, G. Shao, C. Jeynes, R.P. Webb, R.M. Gwilliam, G. Boudreault, D.M. Astill, W.Y. Liang, *Appl. Phys. Lett.* **82**, 236 (2003).

[7] N. Peng, C. Jeynes, R.M. Gwilliam, K.J. Kirkby, R.P. Webb, G. Shao, D.M. Astill, W.Y. Liang, *IEEE Trans. Appl. Supercond.* **15**, 3265 (2005).

[8] S. Soltanian, Ph.D. Thesis, University of Wollongong, Institute for Superconducting & Mectronic Materials, Faculty Engineering, Australia 2004.

[9] G. Karapetrov, M. Iavarone, W.K. Kwok, G.W. Crabtree, D.G. Hinks, *Phys. Rev. Lett.* **86**, 4374 (2001).

[10] G.R. Bollinger, H. Suderow, S. Vieira, *Phys. Rev. Lett.* **86**, 5582 (2001).

[11] P. Seneor, C.T. Chen, N.C. Yeh, R.P. Vasquez, L.D. Bell, C.U. Jung, M.S. Park, H.J. Kim, W.N. Kang, S.I. Lee, *Phys. Rev. B* **65**, 012505 (2001).

[12] M. Xu, Z. Xiao, Y. Takano, T. Hatano, D. Fujita, *Physica C* **412-414**, 283 (2004).

[13] M. Xu, Z. Xiao, Y. Takano, T. Hatano, D. Fujita, *Thin Solid. Films* **464-465**, 61 (2004).

[14] M. Iavarone, G. Karapetrov, A.E. Koshelev, W.K. Kwok, G.W. Crabtree, D.G. Hinks, R. Cook, W.N. Kang, E.M. Choi, H.J. Kim, S.I. Lee, *Physica C* **385**, 215 (2003).

[15] J. Piekoszewski, W. Kempiński, J. Stankowski, F. Prokert, E. Richter, J. Stanisławski, Z. Werner, W. Szymczyk, *Acta Phys. Pol. A* **106**, 861 (2004).

[16] J. Piekoszewski, W. Kempiński, B. Andrzejewski, Z. Trybuła, L. Piekara-Sady, J. Kaszyński, J. Stankowski, Z. Werner, E. Richter, F. Prokert, J. Stanisławski, M. Barlak, *Vacuum* **78**, 123 (2005).

[17] B. Andrzejewski, W. Kempiński, Z. Trybuła, J. Kaszyński, Sz. Łoś, J. Piekoszewski, J. Stanisławski, M. Barlak, J. Jagielski, R. Grötzschel, E. Richter, *Cryogenics* **47**, 267 (2007).

[18] J. Piekoszewski, W. Kempiński, M. Barlak, J. Kaszyński, J. Stanisławski, B. Andrzejewski, Z. Werner, L. Piekara-Sady, E. Richter, J. Stankowski, R. Grötzchel, Sz. Łoś, *Vacuum* **81**, 1398 (2007).

[19] J. Piekoszewski, W. Kempiński, B. Andrzejewski, Z. Trybuła, J. Kaszyński, J. Stankowski, J. Stanisławski, M. Barlak, J. Jagielski, Z. Werner, R. Grötzschel, E. Richter, *Surf. Coat. Technol.* **201**, 8175 (2007).

[20] J. Piekoszewski, W. Kempiński, M. Barlak, Z. Werner, Sz. Łoś, B. Andrzejewski, J. Stankowski, L. Piekara-Sady, E. Składnik-Sadowska, W. Szymczyk, A. Kolitsch, R. Grötzschel, W. Starosta, B. Sartowska, *Surf. Coat. Technol.* **203**, 2694 (2009).

[21] R.J. Hamers, R.M. Tromp, J.E. Demuth, *Phys. Rev. Lett.* **56**, 1972 (1986).

[22] O. Fischer, M. Kugler, I. Maggio-Aprile, Ch. Berthod, Ch. Renner, *Rev. Mod. Phys.* **79**, 367 (2007).

[23] T.W. Heitmann, S.D. Bu, D.M. Kim, J.H. Choi, J. Giencke, C.B. Eom, K.A. Regan, N. Rogado, M.A. Hayward, T. He, J.S. Slusky, P. Khalifah, M. Hass, R.J. Cava, D.C. Larbalestier, M.S. Rzchowski, *Supercond. Sci. Technol.* **17**, 237 (2004).